Capacity Maximization through Depreciation of Carrier Frequency Offset and Sampling Timing Offset in MIMO OFDM Systems

[1]PinkeyRoshan K P V, [2]Dr.D.Sridharan ,

[1]PG scholar, [2] Professor, Department of Electronics & Communication Engineering,
[1]Department of Electronics and Communication Engineering,
[1]Anna University, Chennai, India

ABSTRACT : The MIMO OFDM system has become the superior wireless transmission technique in high speech wireless communication systems. MIMO OFDM has been chosen as the air interface technique for LTE (Long Term Evolution) standard. OFDM system is sensitive to synchronization errors generated by multipath delay, Doppler shift and oscillator instability. In this paper, we address the synchronization problem in non-continuous scenario and propose a block type pilot based synchronization algorithm to suppress the STO (Sampling Timing Offset) and CFO (Carrier Frequency Offset). The pilot pattern used here is CAZAC (Constant Amplitude Zero Autocorrelation) sequence, which is also exploited in LTE Advanced standard. Since the proposed method is a parallel processing, different bands could experience different synchronization errors. Simulation results show the proposed method can significantly improve system performance and has smooth performance when synchronization errors vary. The capacity maximization for the different wireless channels like AWGN, reileigh and Rician channels are estimated using modified Water filling algorithm.

Index Terms **–MIMO OFDM, CAZAC, Long term evolution, Sampling Timing Offset, Carrier frequency Offset, Reileigh, Rician, Water filling algorithm.**

I. INTRODUCTION

In order to meet the demand for high speed wireless communications, ITU has initiated the standardization process of IMT-Advanced. According to the performance requirements defined, future IMT-Advanced systems can support up to 1 Gbps in static as well as pedestrian environments, and 100 Mbps in high-speed mobile environment. To achieve the ambitious performance goals of IMT-Advanced mobile system, 3GPP has completed its LTE standards family Release 8, which will be further improved to LTE-Advanced standards as candidate technical standard for IMT-Advanced systems. In both standards, OFDM has been selected as the air interface technique. Furthermore, according to the existing spectrum allocation policies and the fact that existing spectrum resource in the low frequency band (< 4 GHz) is scarce, CA, a technique that aggregates multiple component bands into an overall wider bandwidth, is proposed to support wide bandwidth transmission in LTE-Advanced standard. In this paper, we focus on the non-continuous CA since it has many advantages, such as flexibility of spectrum assignment.

MOTIVATION

Specifically, the power of a multi-input multi-output MIMO CR system for maximization of the opportunistic system throughput under transmit power, probability of false alarm, and probability of missed detection constraints. To this end, we propose a new transmission protocol which allows the MIMO user to simultaneously perform data transmission and spectrum sensing on different spatial sub-channels. Since finding the global optimal solution of these problems entails a very high complexity, we develop two iterative algorithms that are based on the concept of alternating optimization and solve only convex sub problems in each iteration. Thus, the complexity of these algorithms is low, and we prove their convergence to a fixed point analytically. Simulation results show that the developed algorithms closely approach the global optimal performance and achieve significant performance gains compared to baseline schemes employing equal powers or equal sensing times in all sub-channels.

A fast linear minimum mean square error (LMMSE) channel estimation method has been proposed for Orthogonal Frequency Division Multiplexing (OFDM) systems. In comparison with the conventional LMMSE channel estimation, the proposed channel estimation method does not require the statistic knowledge of the channel in advance and avoids the inverse operation of a large dimension matrix by using the fast Fourier transform (FFT) operation. Therefore, the computational complexity can be reduced significantly. The normalized mean square errors (NMSEs) of the proposed method and the conventional LMMSE estimation have been derived. Numerical results show that the NMSE of the proposed method is very close to that of the conventional LMMSE method, which is also verified by MATLAB simulation. In addition, computer simulation shows that the performance of the proposed method is almost the same with that of the conventional LMMSE method in terms of bit error rate (BER).

CARRIER FREQUENCY OFFSET

However, OFDM system is sensitive to synchronization errors, such as CFO and STO. Inaccurate synchronization will break the orthogonality among subcarriers and introduce ICI (Inter-Carrier-Interference) into received signal, which will lead to serious performance degradation. Furthermore, in non-continuous CA scenario, signals transmitted on different component bands always experience different synchronization errors, which makes synchronization much more difficult. There have been many previous works on synchronization problem. A timing synchronization algorithm was discussed but CFO compensation method wasn't considered. CFO compensation methods are proposed. These frequency synchronization methods can be classified as two groups. The first is called feedback method, which will increase the transmission overhead and possibly cause outdated estimation in time-varying scenario. An alternative is to achieve synchronization via signal processing at the receiver without the help of a control channel, such as [11]. SIC (Successive Interference Cancellation) as well as PIC (Parallel Interference Cancellation) methods were raised. In these methods, the received signals are classified as reliable group and unreliable group.

The reliable signals are directly detected while the unreliable signals are detected after the cancellation of the MAI (Multi-Access Interference) effects due to the reliable signals. Inverse interference matrix method, was discussed. Unfortunately, the methods need perfect multiple CFOs estimation, which is impossible in practical system. And our previous algorithms proposed didn't consider timing offset. Furthermore, all the methods mentioned above are applied in non-CA system, and to our best knowledge, there are few papers about the synchronization problems in CA system. In this paper, we put our attention on the synchronization problems in non-continuous CA system and proposed a block type pilot based synchronization errors suppression algorithm. We suppose the coarse timing synchronization has already been done before we perform the proposed algorithm and the residual timing offset can be reduced within one sampling time period.

SAMPLING TIMING OFFSET

Correlation of the pilot block is used to estimate the STO. Interference estimation is followed after STO estimation. In this stage, pilot block are exploited to estimate the ICI components directly. Then we make suppression by inverse matrix method. Since block type pilot is a common pilot pattern in wireless communications, this method can be easily extended to other systems.

VARIOUS TECHNIQUES

The techniques such as OFDM gained a lot of attention for wireless mobile communications. Indeed, in cyclic prefix (CP), OFDM systems easily equalize time-invariant multipath channels by 1-tap equalizers. However, the request for communications with high mobility suggests that future OFDM designs should take into account also the Doppler spread associated with time-varying wireless channels. This scenario complicates the equalization, because a channel generates Inter symbol Interference thus destroying the orthogonality among OFDM data. We assume that the equalizer does not make use of the virtual subcarriers, which contain little signal power, and could also be affected by interference originated from adjacent transmissions. Moreover, we assume that is known to the receiver. The Optimal LMMSE Equalizer algorithm is used at the receiver of the OFDM system to improve the bit error rate. Consider the MIMO channel model given in Eqn.(1) where the *N* data sub streams are mixed by the channel matrix. The Optimal LMMSE equalizer can be applied to decouple the *N* sub streams.

The Optimal LMMSE equalization matrices are $(H^*H+\frac{1}{SNR}I)^{-1}H^*$. The above equation can be extended to the received Signal $(H^*H+\frac{1}{SNR}I)^{-1}H^*$.

In a 2×2 MIMO channel, consider that we have a transmission sequence, for example {x1, x2,x3, x4}, In normal transmission, we will be sending x1 in the first time slot, x2 in the second time slot, x3 and so on. However, as we now have 2 transmit antennas, we may group the symbols into groups of two. In the first time slot, send x1 and x2 from the first and second antenna. In second time slot, send x3 and x4 from the first and second antenna; send x5 and x6 in the third time slot and so on. Notice that as we are grouping two symbols and sending them in one time slot, we need only 'n' time slots to complete the transmission hence the data rate is doubled. This forms the simple explanation of a probable MIMO transmission scheme with 2 transmit antennas and 2 receive antennas.

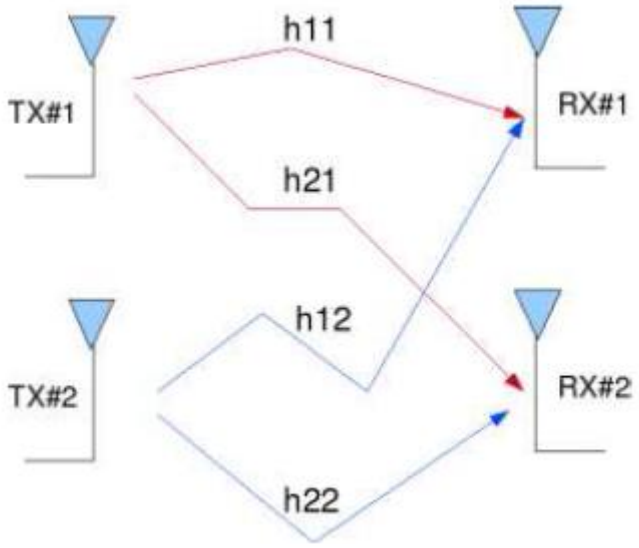

Fig 1.1 Transmit and 2 Receive (2×2) MIMO Channel

In this paper, this has been that the channel is flat fading, it means that the multipath channel has applied on the communication. So, the operation reduces to a simple multiplication and the channel experience by each transmit antenna is independent from the channel experienced by other transmit antennas. For the i^{th} transmit antenna to j^{th} receive antenna, each transmitted symbol gets multiplied by a randomly varying complex numMSE $h_{i,j}$. As the channel under consideration is a Rayleigh channel, the real and imaginary parts of $h_{i,j}$ are Gaussian distributed having mean $\mu h_{i,j}$ and variance σ^2 $h_{i,j}$ =QR . The channel experienced between each transmit to the receive antenna is independent and randomly varying in time.

On the receive antenna, the noise n has the Gaussian probability density function with is used to calculate the CCD,

$$P(n) = \frac{1}{\sqrt{2\pi\sigma^2}} e^{\frac{-(n-\mu)^2}{2\sigma^2}} \text{ with } \mu = 0 \text{ and } \sigma^2 = \frac{N}{2}$$

Explore the relationship of Optimal Linear minimum mean square error (OLMMSE) versus equalizer length. Using the stationary result above we derive a normal equation similar to the one for a single carrier QAM transmission system. Some earlier results have been published on this problem, but only for special cases where the correlation matrix can be easily inverted. Some authors use gradient methods to find the optimal equalizer length for LMS equalizers dynamically. To our knowledge, the explicit closed form expression of Optimal LMMSE versus equalizer length for general cases has not earlier been published. Since the implementation complexity and system latency are directly related to equalizer length, this result has both theoretical and practical value. Equalizer minimizes the error between actual output and desired output by continuous Blind is a digital signal processing technique in which the transmitted signal is inferred from the received signal. Two difficulties arise when the signal in (2) is transmitted over a dispersive channel. One difficulty is that channel dispersion destroys the orthogonality between subcarriers and causes inter carrier interference (ICI). In addition, a system may transmit multiple OFDM symbols in a series so that a dispersive channel causes inter symbol interference (ISI) between successive OFDM symbols. The insertion of a silent guard period between successive OFDM symbols would avoid ISI in a dispersive environment but it does not avoid the loss of the subcarrier orthogonality.

Peled and Ruiz solved this problem with the introduction of a cyclic prefix. This cyclic prefix both preserves the orthogonality of the subcarriers and prevents ISI between successive OFDM symbols. Therefore, equalization at the receiver is very simple. This often motivates the use of OFDM in wireless systems.

$$p_t^k = e^{-j\frac{2\pi\Delta k}{N_k}}$$

The cyclic prefix, illustrated in Figure, works as follows. Between consecutive OFDM signals a guard period is inserted that contains a cyclic extension of the OFDM symbol. The OFDM signal (2) is extended over a period Δ so that

$$s(t) = \frac{1}{\sqrt{N}} \sum_{K=0}^{N-1} X_k e^{j2\pi f_k t} \qquad -\Delta < t < NT \tag{5}$$

The signal then passes through a channel, modeled by a finite-length impulse response limited to the interval $(0, \Delta h)$. If the length of the cyclic prefix Δ is chosen such that $\Delta > \Delta h$ the received OFDM symbol evaluated on the interval [0, NT], ignoring any noise effects, becomes

$$r(t) = s(t) * h(t) = \frac{1}{\sqrt{N}} \sum_{k=0}^{N-1} H_k x_k e^{j2\pi f_k t}, \qquad 0 < t < NT, \tag{6}$$

where

$$H_k = \int_0^{\Delta_h} h(\tau) e^{j2\pi f_k \tau} d\tau \tag{7}$$

The Fourier transform of h(t) evaluated at the frequency f_k. Note that within this interval the received signal is similar to the original signal except that H_kX_k modulates the k^{th} subcarrier instead of X_k. In this way the cyclic prefix preserves the orthogonality of the subcarriers.

Equation (6) suggests that the OFDM signal can be demodulated as described in the previous section, taking an FFT of the sampled data over the interval [0,NT], ignoring the received signal before and after $0 < T \leq NT$ $0 < T \leq NT$. The received data (disregarding additive noise) then has the form

$$y_k = H_k X_k, \; k=0,....N-1 \tag{8}$$

The received data in Equation (8) can be recovered with N parallel one-tap equalizers. This simple channel equalization motivates the use of a cyclic prefix and often the use of OFDM itself. Because we ignore the signal within the cyclic prefix this prefix also acts as the above mentioned silent guard period preventing ISI between successive OFDM symbols. The use of a cyclic prefix in the transmitted signal has the disadvantage of requiring more transmit energy.

The loss of transmit energy (or loss of signal-to-noise ratio (SNR) due to the cyclic prefix is

$$\mathrm{E}_{\mathrm{loss}} = \frac{NT}{NT + \Delta}. \tag{9}$$

This is also a measure of the bit rate reduction required by a cyclic prefix. That is, if each subcarrier can transmit b bits, the overall bit rate in an OFDM system is $NB(NT + \Delta)$ bits per second as compared to the bit rate of b/t in a system without a cyclic prefix. If latency requirements allow, these losses can be made small by choosing a symbol period NT much longer than the length of the cyclic prefix Δ.

CHANNEL NOISE (AWGN)

However, this paper has been mention a few channel impairments that are important for OFDM. OFDM systems often experience not only channel dispersion as addressed above, but also additive white Gaussian noise (AWGN), Doppler spreading and synchronization errors. Many of these impairments can be modelled as AWGN if they are relatively small. Synchronization errors such as carrier frequency offsets, carrier phase noise, sample clock offsets and symbol timing offsets are discussed.

The inclusion of Gaussian noise in the signal model (2) yields a received OFDM signal $r(t) = s(t) * h(t) + n_t(t)$ and Equation (8) extended with a noise term becomes

$$y_k = H_k x_k + n_k, \qquad k = 0, \ldots, N-1, \tag{10}$$

where, n_k is the FFT of the sampled noise terms $n_t(nT)$,n=0,..,N-1 . If the received noise $n_t(t)$ is white, the noise n_k after the FFT will also be white.

In a fading channel the channel variations affect the performance of the OFDM system. For a fixed sampling period, the OFDM symbol length increases with the numMSE of subcarriers and so do its sensitivity to channel variations. To illustrate the effects, consider an OFDM system in a flat-fading channel, a channel with a time-varying

one-tap impulse response a(t). The transmitted OFDM signal is multiplied with this time-varying scalar which yields the received r(t)=a(t) s(t). The multiplication appears as a convolution in the frequency domain causing spreading of the subcarriers and, consequently, ICI.

The sampled signal after the DFT is of the form

$$y_l = \sum_{k=0}^{N-1} x_k A(k-l), \qquad (11)$$

where A(k-1) is the DFT of the now time-varying channel tap n(T),n=0,..,N-1.

In some cases the above spreading may be desirable as it is a way to introduce diversity. A frequency domain channel equalizer can exploit such diversity. Other systems requiring orthogonality between subcarriers may suffer from the spreading. For a fixed sampling time the ICI due to the Doppler spreading increases with the numMSE of carriers. Using a central limit theorem argument, characterizes the effect of the ICI as an additive Gaussian noise with a variance that increases with the numMSE of subcarriers and with the maximum Doppler frequency. This noise is correlated in time, but white across subcarriers. The ICI leads to an error floor which may be unacceptable. Antenna diversity or coding are suggested to reduce this error floor.

RECEIVER

The receiver basically does the reverse operation to the transmitter. The guard period is removed. The FFT of each symbol is then taken to find the original transmitted spectrum. The phase angle of each transmission carrier is then evaluated and converted back to the data word by demodulating the received phase. The data words are then combined back to the same word size as the original data.

SUMMARY

However, OFDM system is sensitive to synchronization errors, such as CFO and STO. Inaccurate synchronization will break the orthogonality among subcarriers and introduce ICI (Inter-Carrier-Interference) into received signal, which will lead to serious performance degradation. Furthermore, in noncontinuous CA scenario, signals transmitted on different component bands always experience different synchronization errors, which makes synchronization much more difficult. There have been many previous works on synchronization problem. A timing synchronization algorithm was discussed but CFO compensation method wasn't considered. Correlation of the pilot block is used to estimate the STO. Interference estimation is followed after STO estimation. In this stage, pilot block are exploited to estimate the ICI components directly.

II. PROPOSED SYSTEM

CFO AND STO ERROR MINIMIZATION USING CAZAC SEQUENCE

This paper has been the synchronization problem in non-continuous scenario and propose a block type pilot based synchronization algorithm to suppress the STO (Sampling Timing Offset) and CFO (Carrier Frequency Offset). The pilot pattern used here is CAZAC (Constant Amplitude Zero Autocorrelation) sequence, which is also exploited in LTE Advanced standard. Since the proposed method is a parallel processing, different bands could experience different synchronization errors. Simulation results show the proposed method can significantly improve system performance and has smooth performance when synchronization errors vary.

CAPACITY MAXIMIZATION USING MODIFIED WATER-FILLING ALGORITHM

In present correspondence we develop proposed water filling algorithm for MIMO fading channel (Rayleigh Fading channel). Orthogonal Frequency Division Multiplexing (OFDM) becomes the chosen modulation technique for wireless communication. Multiple access points or small base stations send independent coded information to multiple mobile terminals through orthogonal Code division multiplexing channels. MIMO OFDM is a promising high data rate interface technology. It is well known the capacity of MIMO OFDM can be significantly enhanced by employing a proper power budget allocation in wireless cellular network.

The singular value decomposition and water filling algorithm have been employed to measure the performance of MIMO OFDM integrated system. When Nt transmit and Nr represented antennas are employed, outage capacity is increased. In MIMO OFDM we transmit different stream of data through different antennas. We show that as we increase the power budget in the water filling algorithm the mean capacity of the system increased.

ADVANTAGES OF PROPOSED SYSTEM

- OFDM makes resourceful utilization of the spectrum by overlapping. By dividing the channel into narrowband flat fading sub channels, OFDM is more resistant to frequency selective fading than single carrier systems.
- It can easily adapt to severe channel conditions without complex time-domain equalization.
- It reduces ISI and IFI through use of a cyclic prefix and fading caused by multipath propagation.
- Using sufficient channel coding and interleaving lost symbols can be recovered.
- Channel equalization becomes simpler than by using adaptive equalization techniques with single carrier systems.
- OFDM is computationally capable by using FFT techniques to implement the modulation and demodulation functions.
- It is less sensitive to sample timing offsets than single carrier systems are.
- It is robust against narrow-band co-channel interference.
- Unlike conventional FDM, tuned sub-channel receiver filters are not required.
-

SUMMARY

A block type pilot based synchronization algorithm to suppress the STO (Sampling Timing Offset) and CFO (Carrier Frequency Offset). The pilot pattern used here is CAZAC (Constant Amplitude Zero Autocorrelation) sequence, which is also exploited in LTE Advanced standard. OFDM is computationally capable by using FFT techniques to implement the modulation and demodulation functions. In present correspondence we develop proposed water filling algorithm for MIMO fading channel (Rayleigh Fading channel). Orthogonal Frequency Division Multiplexing (OFDM) becomes the chosen modulation technique for wireless communication.

AbbreviationsandAcronyms(Heading2)

Defineabbreviationsandacronymsthefirsttimetheyareusedinthetext,evenaftertheyhavebeendefinedintheabstract.Abbreviationssuchas IEEEandSIdonothavetobedefined.Donotuseabbreviationsinthetitleorheadsunlesstheyareunavoidable.

III. SYSTEM MODEL

The carrier frequency of the k^{th} component band is denoted as f_c^k and the subcarrier amount of the k^{th} component band is Nk. Without loss of generality, we suppose K component bands are exploited in this communication system. In the Fig 3.1 shows the simplified block diagram of the OFDM based non-continuous carrier aggregation system.

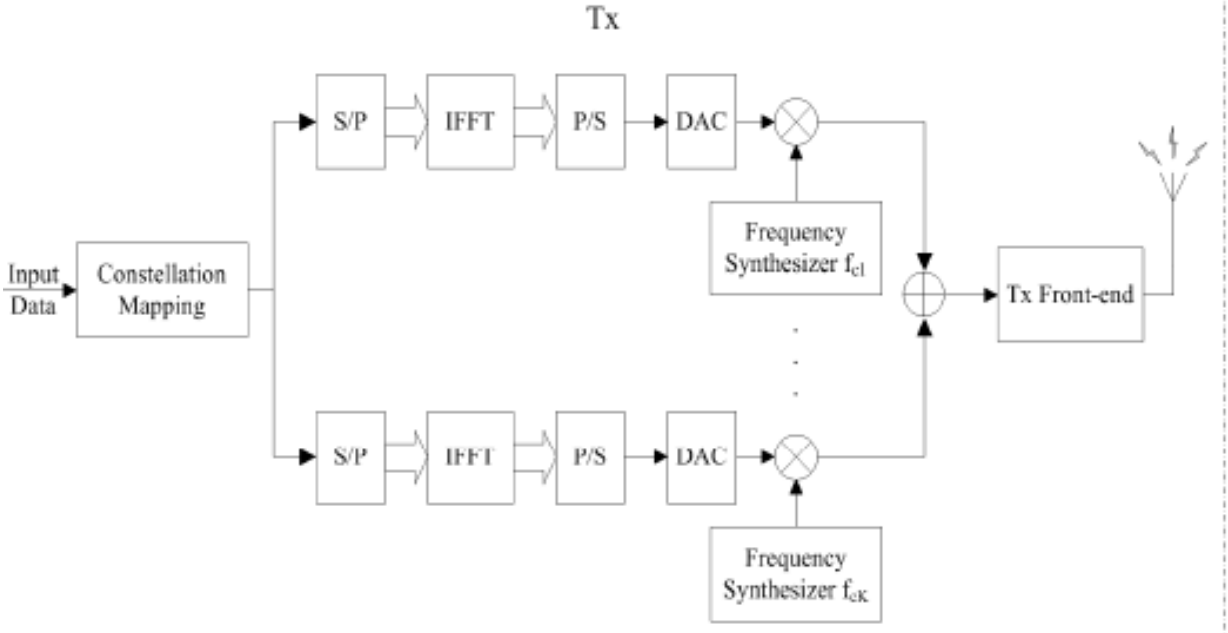

Fig 3.1 Block diagram of OFDM (transmitter side) based non-continuous CA system

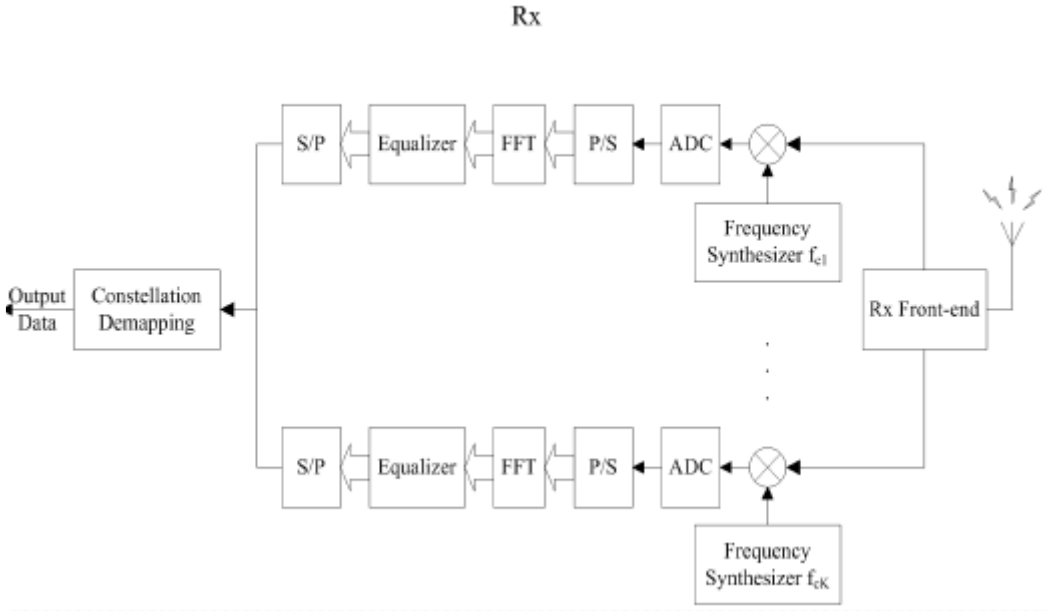

Fig.3.2 Block diagram of OFDM (receiver side) based non-continuous CA system

Here the vector $d^k=[d_0^k,d_1^k,....d_{Nk-1}^k]^T$, (k=1, 2, 3 …, K) denotes the transmitted data on the k^{th} component band. Then the output of the N_k.-IFFT is

$$s^k(n)=\frac{1}{\sqrt{N_k}}\sum_{i=0}^{N_k-1}d_i^k\cdot e^{j2\pi ni/N_k}. \qquad (1)$$

The base band signal will be modulated to the transmission band with the carrier frequency f_c^k which is generated by the transmitter frequency synchronizer at the up-converter. Here we consider each signal experiences a frequency selective fading channel with the time domain impulse response $h_k(n)$ (k=1, 2, 3 …,K).

Then the received signal is the superposition of signals from all active component bands and can be written as

$$r(t)=\sum_{k=1}^{K}[(s^k(t).e^{j2\pi f_c^k t})\otimes h^k(t)+v^k(t)] \qquad (2)$$

Where " $\otimes$ " denotes convolution and $v_k(t)$ is the AWGN on the k^{th} component band.

To extract the transmitted signal $r_k(t)$ on the k^{th} component band, the generated signal will pass through a low-pass filter and cancel the signals from the other component bands. Through N_k-FFT processing, the output of the l^{th} subcarrier on the k^{th} component band is

$$Y_i^k=\frac{1}{N_k}\sum_{n=0}^{N_k-1}\sum_{i=0}^{N_k-1}d_i^kH_i^ke^{j2\pi ni\frac{i}{N_k}}e^{-j2\pi ni\frac{i}{N_k}}=d_i^kH_i^k \qquad (3)$$

Where H_i^k denotes the frequency domain channel response of the k^{th} component band.

3.1 INFLUENCE OF SYNCHRONIZATION ERRORS

To start the influence of inaccurate synchronization, multiple CFOs and STOs will be introduced into the received signals. CFO and STO of the k^{th} component band are denoted as Δf_e^k and Δt_e^k respectively.

After transmitted through fading channels, the CFOs and channel fading corrupted time domain signal can be written as

$$r(t)=\sum_{k=1}^{K}[(s^k(t).e^{j2\pi f_c^k t+\forall f_q^k})\otimes h^k(t)+v^k(t)] \qquad (4)$$

For non-continuous CA, different component bands are usually separated by sufficient bandwidth, so the interference between them can be negligible. The STO corrupted received signal can be written as

$$r^k(n)=\sum_{i=1}^{N_K-1}[(s^k(t).e^{j2\pi\forall f_q^k t})\otimes h^k(t)+v^k(t)]_{t=nt_s+\forall t_q^k}$$

$$Y_t^k=\frac{1}{N_k}\sum_{i=0}^{N_k-1}\sum_{n=0}^{N_k-1}d_i^kH_i^kP_k^ie^{j2\pi ni\frac{i}{N_k}}e^{j\frac{2\pi(nl+n\in_k+\in_k)}{N_k}}e^{-j\frac{2\pi nl}{N_k}}+V_t^k$$

$$=d_i^kH_i^kP_k^iQ_o^k+\sum_{i=0}^{N_k-1}d_i^kH_i^kP_k^iQ_{i-1}^k+V_t^k \qquad (6)$$

where T_s=T/Nk is the sampling period,

T denotes the symbol period,

εk and δk denote the normalized CFO and STO respectively as $p_t^k = e^{-j\frac{2\pi\Delta_k}{N_k}}$

After FFT, Where

$$Q_L^k = \frac{1}{N_k}\sum_{n=0}^{N_k-1} e^{j\frac{2\pi n(L+\varepsilon_k)}{N_k}} e^{j\frac{2\pi\varepsilon_k\delta_k}{N_k}}$$

denotes the interference factor and V_k^l denotes AWGN.

Obviously, we can obtain the matrix expressed frequency domain signal vector according to the above equation

$$= \sum_{l=0}^{\frac{N_K}{2}-1} (-1)^{l+1} \frac{P^k(1+\frac{N_K}{2})}{H^k_{l+\frac{N_K}{2}}}\left(P^K \frac{(l)}{H_l^k}\right)$$

$$= \sum_{l=0}^{\frac{N_k}{2}-1} |P_l^k|^2 |Q_0^k|^2 [P^k(1+\frac{N_K}{2}).(P_l^k)]$$

$$= e^{j\pi\delta_k} \sum_{L=0}^{\frac{N_K-1}{2}} |P^K(l)|^2 |Q_o^k|^2$$

Where

$$\mathbf{R}_\mathbf{V}^k = \left[R_0^k, R_1^k, \ldots, R_{N_k-1}^k\right]^T (R_l^k = d_l^k H_l^k)$$

denotes the received signal vector distorted by channel fading,

$$\mathbf{P}_\mathbf{M}^k = diag(p_0^k, p_1^k, \ldots p_{N_k-1}^k)$$

denotes the phase rotation matrix caused by STO and

$$\mathbf{Q}_\mathbf{M}^k = \begin{bmatrix} Q_0^k & Q_1^k & \cdots & Q_{N_k-1}^k \\ Q_{-1}^k & Q_0^k & \cdots & Q_{N_k-2}^k \\ \vdots & \vdots & \ddots & \vdots \\ Q_{-(N_k-1)}^k & Q_{-(N_k-2)}^k & \cdots & Q_0^k \end{bmatrix} \quad (8)$$

denotes the ICI matrix caused by CFO. The diagonal components in k Q^{KM} are the CPE (Common Phase Error) components and the other components denote the ICI from the corresponding subcarriers.

3.2 SYNCHRONIZATION ERRORS SUPPRESSION ALGORITHM

In this paper has been discuss the proposed block type pilot based synchronization errors suppression algorithm. The pilot pattern used here is the CAZAC sequence, which is one of the strongest candidates as pilot pattern in OFDM system and has been exploited by LTE-Advanced standard. Let *L* to be any positive integer larger than one and *M* to be any numMSE, which is relatively prime with *L*.

Then an example of CAZAC sequence is given as

$$\begin{cases} c_M(n) = e^{j\frac{2\pi M}{L}(n+n\frac{n+1}{2})}, n = 0,1,\ldots,L-1, L\ is\ odd \\ c_M(n) = e^{j\frac{2\pi M}{L}(n+\frac{n^2}{2})}, n = 0,1,\ldots,L-1, L\ is\ even \end{cases} \quad (9)$$

The circular auto-correlation of CAZAC sequence is

$$\sum_{n=0}^{L-1} c_M(n)\cdot c_M(n+\tau)_{\bmod L} = \begin{cases} L, & \tau = 0 \\ 0, & \tau \neq 0 \end{cases} \quad (10)$$

3.2.1 STO ESTIMATION ALGORITHM

In this paper has been discuss the proposed frequency domain STO estimation algorithm to obtain the STO between the practical sampling time and optimum sampling time.

To implement this algorithm, special CAZAC sequence should be exploited, in which pilots spaced by half subcarriers amount should satisfy the following requirement

$$P_l^k = \pm P_{l+N_k/2}^k. \quad (11)$$

Where p_t^k denotes the pilot transmitted on the l^{th} subcarrier of the k^{th} component band.

In OFDM system, since the amount of subcarrier is always an even numMSE, we can obtain the expression of p_t^k as

$$P_l^k = e^{j\frac{2\pi M}{N_k}(l+\frac{l^2}{2})}, l = 0, 1, ..., N_k - 1. \quad (12)$$

Obviously, to satisfy the above requirement, we just need to set M as an odd and N_k as a multiple of 4 (in this scenario, M is naturally relatively prime with N_k). In OFDM system, to achieve high speed FFT/IFFT, subcarrier amount is usually set as exponential times of 2. Thus the above requirement can be achieved by just set M as an odd numMSE.

Therefore

$$\begin{cases} P_l^k = P_{l+N_k/2}^k, if\ l\ is\ odd \\ P_l^k = -P_{l+N_k/2}^k, if\ l\ is\ even \end{cases}, \quad (13)$$

As illustrated in previous section, ICI has the appearance of Gaussian noise. Furthermore, according to the interference self-cancellation algorithm, the pilot pattern used here could alleviate the interference. Therefore, we could treat the interferences as noise and don't consider it.

In this situation, the l^{th} received pilots can be expressed as

$$P^k(l) = P_l^k \cdot H_l^k \cdot p_l^k \cdot Q_0^k. \quad (14)$$

Suppose the frequency domain channel response has already been estimated. Then the correlation can be calculated as follows

$$\begin{aligned} \eta &= \sum_{l=0}^{\frac{N_K}{2}-1} (-1)^{l+1} \frac{P^k(1+\frac{N_K}{2})}{H^k_{l+\frac{N_K}{2}}} \left(P^K \frac{(l)}{H_l^k} \right) \\ &= \sum_{l=0}^{\frac{N_k}{2}-1} |P_l^k|^2 |Q_0^k|^2 [P^k(1+\frac{N_K}{2}).(p_l^k)] \\ &= e^{j\pi\delta_k} \sum_{L=0}^{\frac{N_K-1}{2}} |P^K(l)|^2 |Q_o^k|^2 \end{aligned} \quad (15)$$

Therefore, the STO of the k^{th} component band can be obtained from the phase of η as

$$\delta_k = \arctan(\frac{\mathrm{Im}(\eta)}{\mathrm{Re}(\eta)})/\pi. \quad (16)$$

Since the variation range of arctan(x) is $(-\pi/2, \pi/2)$, the estimation range is (-0.5, 0.5), which fully covered the available value of STO.

3.2.2 INTERFERENCE SUPPRESSION ALGORITHM

After STO estimation, this paper perform interference estimation and then suppress the inaccurate synchronization. Instead of estimating CFOs, which is fairly difficult to get accurate results, we directly estimate the interference components under the aid of the received pilot block. After that, the ICI matrix can be reconstructed by very simple mapping method. Then we can suppress interferences by inverse matrix method and finally improve system performance.

From the expression of Q_L^Kwe can obtain that

$$\begin{aligned} Q_{-L}^k &= \frac{1}{N_k} \sum_{n=0}^{N_k-1} e^{j\frac{2\pi n(-L+\varepsilon_k)}{N_k}} e^{j\frac{2\pi\varepsilon_k\delta_k}{N_k}} \\ &= \frac{1}{N_k} \sum_{n=0}^{N_k-1} e^{j\frac{2\pi n(N_k-L+\varepsilon_k)}{N_k}} e^{j\frac{2\pi\varepsilon_k\delta_k}{N_k}} \\ &= Q_{N_k-L}^k \end{aligned} \quad (17)$$

Therefore, the ICI matrix Q_m^kcan be rewritten as

$$\mathbf{Q}_\mathbf{M}^k = \begin{bmatrix} Q_0^k & Q_1^k & \cdots & Q_{N_k-1}^k \\ Q_{N_k-1}^k & Q_0^k & \cdots & Q_{N_k-2}^k \\ \vdots & \vdots & \ddots & \vdots \\ Q_1^k & Q_2^k & \cdots & Q_0^k \end{bmatrix}. \quad (18)$$

In this paper has been see that Q_m^k the matrix is a circulant matrix with only N_K different components. Therefore,

$$\begin{aligned}\mathbf{Y}_{\mathbf{V}}^{k} &= \begin{bmatrix} Q_0^k & Q_1^k & \cdots & Q_{N_k-1}^k \\ Q_{N_k-1}^k & Q_0^k & \cdots & Q_{N_k-2}^k \\ \vdots & \vdots & \ddots & \vdots \\ Q_1^k & Q_2^k & \cdots & Q_0^k \end{bmatrix} \cdot \mathbf{P}_{\mathbf{M}}^{k} \cdot \begin{bmatrix} R_0^k \\ R_1^k \\ \vdots \\ R_{N_k-1}^k \end{bmatrix} + \mathbf{V}_k \\ &= \begin{bmatrix} R_0^k p_0^k & R_1^k p_1^k & \cdots & R_{N_k-1}^k p_{N_k-1}^k \\ R_1^k p_1^k & R_2^k p_2^k & \cdots & R_0^k p_0^k \\ \vdots & \vdots & \ddots & \vdots \\ R_{N_k-1}^k p_{N_k-1}^k & R_0^k p_0^k & \cdots & R_{N_k-2}^k p_{N_k-2}^k \end{bmatrix} \cdot \begin{bmatrix} Q_0^k \\ Q_1^k \\ \vdots \\ Q_{N_k-1}^k \end{bmatrix}, \\ &\quad + \mathbf{V}_k \\ &= \mathbf{R}_{\mathbf{M}}^{k} \cdot \mathbf{Q}_{\mathbf{V}}^{k} + \mathbf{V}_k \end{aligned} \tag{19}$$

Where

$$\mathbf{Q}_{\mathbf{V}}^{k} = \left[Q_0^k, Q_1^k, \ldots, Q_{N_k-1}^k\right]^T$$

$$\mathbf{R}_{\mathbf{M}}^{k} = \begin{bmatrix} R_0^k p_0^k & R_1^k p_1^k & \cdots & R_{N_k-1}^k p_{N_k-1}^k \\ R_1^k p_1^k & R_2^k p_2^k & \cdots & R_0^k p_0^k \\ \vdots & \vdots & \ddots & \vdots \\ R_{N_k-1}^k p_{N_k-1}^k & R_0^k p_0^k & \cdots & R_{N_k-2}^k p_{N_k-2}^k \end{bmatrix}. \tag{20}$$

The equation (20) as an equations set and the N_k components in Q_M^K as the unknown values. If we can estimate these N_k values by solving this equations set, the Q_M^K matrix can be reconstructed and the interferences of CFO can be suppressed by multiply the inverse Q_M^K matrix with the received signal. Since STO has already been estimated and the pilots are known to receive, R_M^K can be easily calculated. Obviously, k M R is a full rank matrix.

Thus, $(R_M^K)^{-1}$ can be easily constructed and Q_V^K which contains the N^k components in Q_M^K, can be easily estimated by

$$\tilde{\mathbf{Q}}_{\mathbf{V}}^{k} = \left(\mathbf{R}_{\mathbf{M}}^{k}\right)^{-1} \cdot \mathbf{Y}_{\mathbf{V}}^{k} = \mathbf{Q}_{\mathbf{V}}^{k} + \left(\mathbf{R}_{\mathbf{M}}^{k}\right)^{-1} \cdot \mathbf{V}_k . \tag{21}$$

After that, the interference matrix Q_M^K can be reconstructed from the estimated Q_V CFO are highly correlated during the pilot block and the following data blocks.

Therefore, the synchronization errors can be easily suppressed by LS (Least Square) method as

$$\begin{aligned}\mathbf{Y}_{suppressed}^{k} &= \left(\mathbf{P}_{\mathbf{M}}^{k}\right)^{H} \left[\left(\tilde{\mathbf{Q}}_{\mathbf{M}}^{k}\right)^{H} \tilde{\mathbf{Q}}_{\mathbf{M}}^{k}\right]^{-1} \left(\tilde{\mathbf{Q}}_{\mathbf{M}}^{k}\right)^{H} \mathbf{Y}_{\mathbf{V}}^{k} \\ &= \mathbf{R}_{\mathbf{V}}^{k} + \left(\mathbf{P}_{\mathbf{M}}^{k}\right)^{H} \left[\left(\tilde{\mathbf{Q}}_{\mathbf{M}}^{k}\right)^{H} \tilde{\mathbf{Q}}_{\mathbf{M}}^{k}\right]^{-1} \left(\tilde{\mathbf{Q}}_{\mathbf{M}}^{k}\right)^{H} \mathbf{V}_k \end{aligned} \tag{22}$$

Since the interferences from other component bands are ignorable, the synchronization errors of each band could be independent and have few influences on the suppression performance. Therefore, we can use parallel process to suppress the inaccurate synchronization on each band.

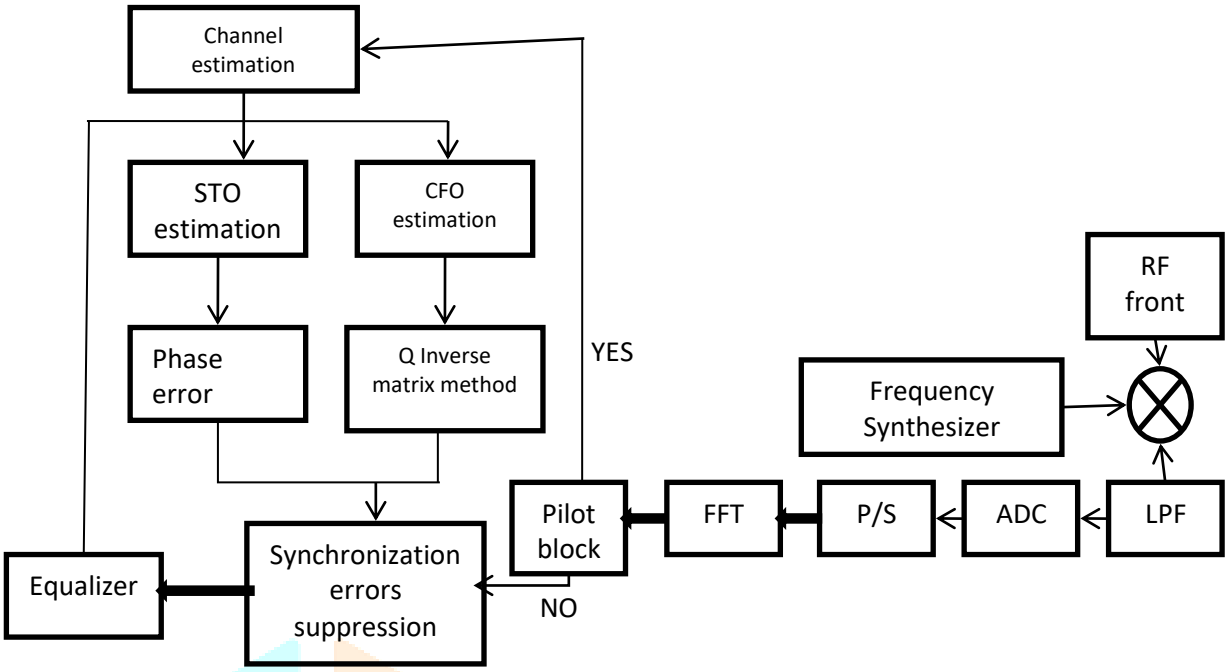

Fig 3.3 Block diagram of synchronization errors suppression algorithm

The whole processing can be described as follows:
(1) When a symbol arrives at the receiver, detect whether this symbol is a pilot symbol:
Yes, go to step (2); No, go to step (5);
(2) Do channel estimation;
(3) Do STO estimation under the aid of channel estimation;
(4) Do Q matrix estimation under the aids of channel estimation results and STO estimation results;
(5) Do inverse-matrix based suppression algorithm;

3.2.3 CAPACITY MAXIMIZATION USING MODIFIED WATERFILLING ALGORITHM

Orthogonal frequency division multiplexing is a popular wireless multicarrier transmission technique. It is a promising candidate for next generation wired and mobile wireless system. The basic principle of OFDM is to split a high data rate stream into a number of low data rate stream so that the lower data rate can be transmitted simultaneously over a number of subcarriers. In OFDM, the amount of dispersion in time caused by multipath delay spread is decreased due to increased symbol duration for lower rate parallel subcarriers. The spectrum of OFDM is more efficient because of the use of closer channel space. Interference is prevented by making all subcarrier orthogonal to one another. MIMO system utilizes space multiplex by using antenna array to enhance the efficiency in the used bandwidth. These systems are defined spatial diversity and spatial multiplexing.

Spatial diversity is known as Tx- and Rx- diversity. Signal copies are transferred from another antenna, or received at more than one antenna. With spatial multiplexing, the system carriers' more than one spatial data stream over one frequency, simultaneously. In subcarriers MIMO-OFDM system, the individual data stream is first passed through an OFDM modulator.

Then the resulting OFDM symbols are launched simultaneously through the transmit antenna. In a receiver side ,the individual received signal are passed through OFDM demodulator .The output of OFDM demodulator are decoded and rearranged to get desired output

3.2.3.1 SPATIAL MULTIPLEXING

The transmission of multiple data stream over more than one antenna is called spatial multiplexing. The advantages of spatial multiplexing is linear capacity gains in relation to the number of transmit antenna

3.2.3.2 MIMO CHANNEL MATRIX

The matrix describes the channel behavior on a particular subcarrier (n) for a particular user (k). Here k and n represents the number of users and subcarrier respectively which as follows-

$$H=\begin{pmatrix} H1,1 & H1,2 \ldots\ldots\ldots H1,n \\ H2,1 & H2,2 \ldots\ldots\ldots\ldots H2,n \\ Hk,1 \ldots\ldots & \ldots\ldots\ldots\ldots Hk,,n \end{pmatrix} \quad (1)$$

Where $H_{k,n}$ is already defined.

3.2.3.3 CAPACITY

Capacity is the measure of maximum information that can be transmitted reliably over a channel. Claude Elwood Shannon developed the following equation for theoretical channel capacity:

$$B \log (1+SNR) \quad (2)$$

It includes the transmission bandwidth B and signal to noise ratio. The Shannon capacity of MIMO system depends on the number of antenna.

For MIMO the capacity is given by the following equation:

$$C_{mimo} = NB (1+SNR) \quad (3)$$

where N is the minimum of N_t (number of transmitting antennas) or N_r (number of receiving antennas.

3.2.3.4 SINGULAR VALUE DECOMPOSITION

The SVD techniques decouples the channel matrix in spatial domain in a similar to the DFT decoupling the channel in the frequency domain. If channel matrix H is the T x R channel matrix.

If H has independent rows and columns, SVD yields:

$$H = U\Sigma Vh$$

where U and V are unitary matrices and Vh is the hermitian of V.

U has dimension of R x R and V has dimension of T x T. If T=R then Σ become a diagonal matrix. If T>R, is made of R x R diagonal matrix followed by T-R zero column. If T<R, it is made of T x T diagonal matrix followed by R – T 0 rows. This operation is called the singular value decomposition of H In case where T ≠ R the number of spatial channels become restricted to minimum to T and R. if the number of transmit antenna > receive antenna U will be an R x R matrix, V will be a T x T matrix and Σ will be made of square matrix of order R followed by T – R zero columns.

The process of water filling algorithm is similar to pouring the water in the vessel. The unshaded portion of the graph represents the inverse of the power gain of a specific channel. The Shadow portion represents the power allocated or the water. The total amount on water filled (power allocated) is proportional to the Signal to Noise Ratio of channel.

Power allocated by individual channel is given by the eq. 1, as shown in the following formula

$$\text{Powerallocated} = \frac{Pt+\sum\frac{1}{Hi}}{\sum channel} - \frac{1}{Hi} \quad (4)$$

where P_t is the power budget of MIMO system which is allocated among the different channels and H is the channel matrix of system.

The capacity of a MIMO is the algebraic sum of the capacities of all channels and given by the formula below.

$$\text{Capacity} = \Sigma \log (1 + PowerAllocated * H)\, ni$$

To maximize the total number of bits to be transported .As per the scheme following steps are followed to carry out the water filling algorithm steps:-

i. Take the inverse of the channel gains.
ii. Water filling has non uniform step structure due to the inverse of the channel gain.
iii. Initially take the sum of the total power P_t and the inverse of the channel gain. It gives the complete area in the water filling and inverse power gain

$$Pt+\sum_{i=1}^{n}\frac{1}{Hi}$$

Decide the initial water level by the formula given below by taking the average power allocated

$$\frac{Pt+\sum_{i=1}^{n}\frac{1}{Hi}}{\sum Channel}$$

The power values of each sub channel are calculated by subtracting the inverse channel gain of each channel

$$\text{Powerallocated} = \frac{Pt+\sum_{i=1}^{n}\frac{1}{Hi}}{\sum Channel} - \frac{1}{Hi}$$

A. OFDM SIMULATION MODEL

Serial to Parallel Conversion the input serial data stream is formatted into the word size required for transmission, e.g. 2 bits/word for QPSK, and shifted into a parallel format. The data is then transmitted in parallel by assigning each data word to one carrier in the transmission.

B. MODULATION OF DATA

The data to be transmitted on each carrier is then differential encoded with previous symbols, then mapped into a Phase Shift Keying (PSK) format. Since differential encoding requires an initial phase reference an extra symbol is added at the start for this purpose. The data on each symbol is then mapped to a phase angle based on the modulation method. For example, for QPSK the phase angles used are 0, 90, 180, and 270 degrees.

C. INVERSE FOURIER TRANSFORM

After the required spectrum is worked out, an inverse Fourier transform is used to find the corresponding time waveform. The guard period is then added to the start of each symbol.

D. GUARD PERIOD

The guard period used was made up of two sections. Half of the guard period time is a zero amplitude transmission. The other half of the guard period is a cyclic extension of the symbol to be transmitted. This was to allow for symbol timing to be easily recovered by envelope detection.

However it was found that it was not required in any of the simulations as the timing could be accurately determined position of the samples. After the guard has been added, the symbols are then converted back to a serial time waveform.

The phenomenon of multipath propagation has contributed significantly towards deterioration of quality of signal received in a wireless communication system. Several techniques for multipath mitigation are in use in the current wireless communication technology standards. With the steady rise in the number of wireless devices active in the environment, the concept of beam forming has gained popularity. When multiple communications are carried out simultaneously, then in multipath environment the interference from different directions will also increase. This multipath propagation causes the signal at the receiver to distort and fade significantly, leading to higher bit error rates (BER). To minimize the interference from different directions, smart antennas can be used at the receivers which form the beam in the direction of the incoming multipath and reject the interference coming from other directions.

In a wireless communication scenario, transmitted signals often propagate via just a few distinct paths, for example via a line-of-sight path between transmitter and receiver and/or via paths that are associated with significant reflectors and diffractors in the environment (such as large buildings or mountains). If the directions of these dominant propagation paths are known at the receiver side, beam forming techniques can be applied, in order to adjust the receiver beam pattern such that it has a high directivity towards the dominant angles of reception. By this means, significant SNR gains can be accomplished in comparison to an antenna array with an omni-directional beam pattern. Such SNR gains due to beam forming techniques are often called antenna gains or array gains in the literature. Similarly, if the directions of the dominant propagation paths are known at the transmitter side, the transmit power can be concentrated within the corresponding angular regions and is not wasted for directions that do not contribute to the received signal.

Beam forming techniques can also be useful, in order to reduce the delay spread of the physical channel caused by multipath signal propagation. To this end, receiver beam pattern is adjusted such that it exhibits nulls in the directions of dominant distant reflectors. Correspondingly, echoes with excessively large delays are eliminated from the received signal.

For comparisons of the computational complexity, the numbers of real multiplications and real additions used for the PAPR reduction are considered. It is well known that –point IFFT modules for the conventional SLM scheme require complex multiplications and complex additions. Considering phase sequence composed of or, complex multiplications in order to generate alternative frequency domain OFDM sequences are not necessary [10]. Since one complex multiplication is accomplished by four real multiplications and two real additions, and one complex addition is achieved by two real additions, the required real multiplications and real additions for the SLM scheme are and , respectively. For the proposed scheme with alternative OFDM sequences, only one IFFT module used with all-pass filters is required. In this case, the computational complexity of an all-pass filter with poles is obtained from the difference equation of the all-pass filters.

Note that the frequency response in the proposed scheme replaces the phase sequence in the SLM scheme. Finally, the OFDM sequence with the minimum PAPR is selected for transmission. The OFDM sequence in (6) corresponds to the circular convolution of the OFDM sequence with impulse response , which is defined as . However, all-pass filters generally perform a linear convolution, so for the all-pass filters to perform the circular convolution, a Cyclic Prefix (CP), a replica of for, is placed at the beginning of the original OFDM sequence . It is removed after passing through the all-pass filters.

3.3 SUMMARY

To start the influence of inaccurate synchronization, multiple CFOs and STOs will be introduced into the received signals. After STO estimation, we perform interference estimation and then suppress the inaccurate

synchronization. Instead of estimating CFOs, which is fairly difficult to get accurate results, we directly estimate the interference components under the aid of the received pilot block.

IV. SIMULATION RESULTS AND DISCUSSION

The simulation parameters.

Non-Continuous CA system	
Component Band Amount	4
Subcarrier Amount per Component Band	512
Subcarrier Spacing	15 *kHz*
Component Bandwidth	7.5 *MHz*
Modulation Scheme	16 QAM
Sub-frame Structure	1 Pilot Symbol + 5 Data Symbols
Sampling Rate	Nyquist Sampling Rate
Sampling Period	130 *ns*
CP Length	64
Channel Model	AWGN & ITU Ped-B

The ITU Ped-B (Pedestrian B) channel is modeled as a tapped-delay line with 6 non-uniform delay taps. The channel gains of these taps are [0, -0.9, -4.9, -8.0, -7.8, -23.9] dB and the delays of these taps are [0, 200, 800, 1200, 2300, 3700] ns respectively. We also assume that the synchronization errors are quasi static during the pilot block and the following 5 data blocks. In the following simulations, the normalized STO of each band is uniformly distributed in [0, 0.5] and the normalized CFO of each band is uniformly distributed in [-0.05, 0.05]. Fig. 4.1 shows the MSE (Mean Square Error) performance of the proposed STO estimation algorithm.

The results are evaluated in AWGN and ITU Ped-B scenarios. According to the simulation results, the MSE of the proposed algorithm can be reduced around 10-4 level. That means the maximum residual phase rotation is about 3.6degree, which is a fairly small value and could cause little performance degradation.

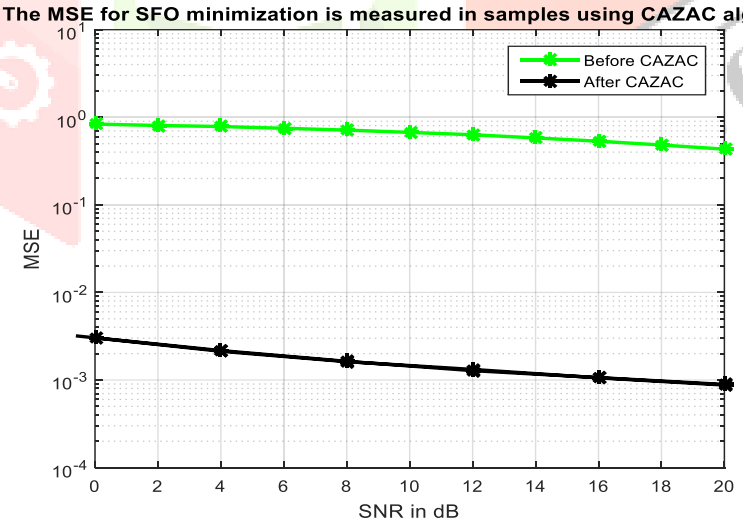

Fig 4.1The MSE for SFO Minimization is measured in samples using CAZAC algorithm

This paper has been select the algorithm proposed as comparison and chosen 5, 10, and 50 as the bandwidth of the banded-matrix. Fig. 4.1 shows the MSE performance in AWGN channel and Fig. 4.2 shows the MSE performance in Ped-B channel.

Comparing the simulation results, we can see that due to the co-effects of CFO and STO, the MSE performance will be degraded seriously. If banded matrix suppression method is used, when the bandwidth is small (for example, τ=5, 10), a serious error floor phenomenon occurs in high SNR range.

Fortunately, the proposed suppression algorithm can significantly improve system performance in both channels and can achieve the best suppression performance. To check the impact of CFO magnitude, we simulate in another scenario, where the normalized CFO varies from 0 to 0.5.

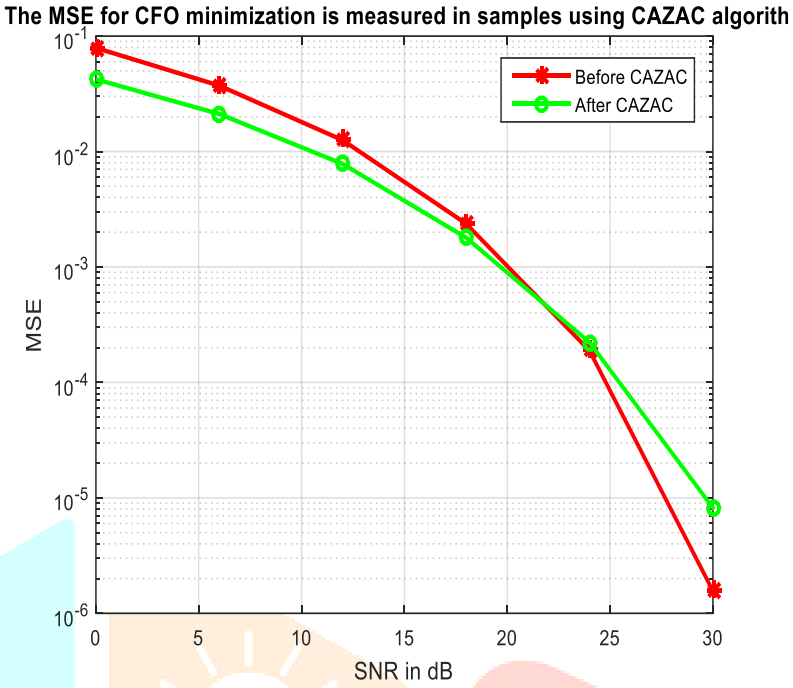

Fig 4.2: The MSE for CFO Minimization is measured in samples using CAZAC

We select the algorithm proposed as comparison and choosed 5, 10, 50 as the bandwidth of the banded-matrix. Fig.4. 2 shows the MSE performance in AWGN channel and Fig. 3 shows the MSE performance in Ped-B channel.

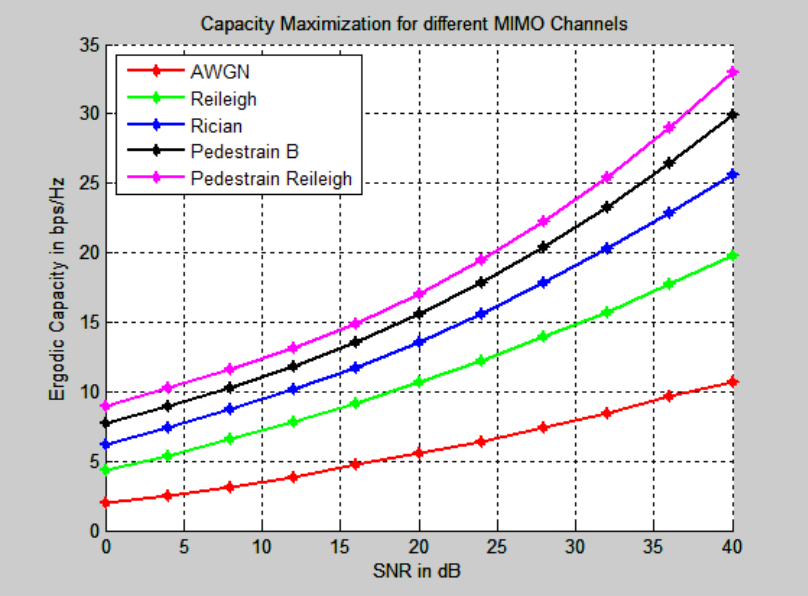

Fig 4.3 Capacity maximization for different mimo channel

Comparing the simulation results, we can see that due to the co-effects of CFO and STO, the MSE performance will be degraded seriously. If we used banded matrix suppression method, when the bandwidth is small (for example, τ=5, 10), a serious error floor phenomenon occurs in high SNR range.

The capacity maximization for the different wireless channels like AWGN, reileigh and Rician channels are estimated using modified Water-filling algorithm in Fig 4.3. The guard bit interval in the system comes with the issues of PAPR and this will be minimized by providing proper synchronization between communication systems. Fig.4. 3 shows the MSE performance in AWGN channel when SNR=10dB the MSE performance in Ped-B channel when SNR=10dB. From the simulation results, we can see that the proposed algorithm almost has the same performance when CFO increases. Thus it is robust to the variance of CFO.

When multiple communications are carried out simultaneously, then in multipath environment the interference from different directions will also increase. This multipath propagation causes the signal at the receiver to distort and

fade significantly, leading to higher bit error rates (BER). To minimize the interference from different directions, smart antennas can be used at the receivers which form the beam in the direction of the incoming multipath and reject the interference coming from other directions.

SUMMARY

Fortunately, the proposed suppression algorithm can significantly improve system performance in both channels and can achieve the best suppression performance. To check the impact of CFO magnitude, we simulate in another scenario, where the normalized CFO varies from 0 to 0.5. Fig. 3 shows the MSE performance in AWGN channel when SNR=10dB and Fig. 7 shows the MSE performance in Ped-B channel when SNR=10dB. From the simulation results, we can see that the proposed algorithm almost has the same performance when CFO increases. Thus it is robust to the variance of CFO.

V. CONCLUSION

With the implementation of MIMO-OFDM, the probability that the transmission arrives at the receiver with little or no error is greatly increased compared to the rest of the transmission techniques. In this system, the capacity is increased significantly by transmitting the different streams of data through different antennas at a same carrier frequency. A new PAPR reduction scheme for OFDM systems was proposed in this paper. It was found that with simple all-pass filters the proposed scheme could significantly reduce the computational complexity, at the cost of slightly worse PAPR reduction performance over the conventional SLM scheme, without BER performance degradation. We focus on the synchronization problems in non-continuous CA OFDM system and propose a novel block type pilot based synchronization errors suppression algorithm.

Unlike other STO estimation algorithms, the proposed method exploits special kind of CAZAC sequence, which abides by the rule of interference self-cancellation and can improve estimation accuracy. Furthermore, the proposed algorithm could directly estimate the interference components without CFO estimation. Thus, system complexity can be reduced. Most of all, the synchronization errors of each band could be independent, which is more close to practical situation. According to the simulation results, the proposed algorithm could significantly improve system performance and achieve smooth performance when synchronization errors vary. Since the CAZAC sequence pilot pattern is defined in LTEAdvanced standard, this algorithm can be treat as a candidate method in LTE-Advanced system and other block type pilot based systems.

One first introduces the general landscape of the next generation of wireless communication systems (5G), including its driver and requirements, and the candidate technologies that might help to achieve its intended goals. The following areas, which the author considers to be of particular relevance for 5G, are then introduced: detection of and access to free spectrum over bands of an heterogeneous nature, extreme densification of networks (massive base station deployments), extreme increase in the number of antennas in transmitter arrays and their interaction with a novel waveform, integration of both wireless and optical sides of telecom networks, and study of wireless networks using the magnifying glass provided by complex systems science.

LIST OF ABBREVATIONS

CFO	Carrier Frequency Offset
STO	Sampling Riming Offset
CAZAC	Constant Amplitude Zero Auto Correlation
CP	Cyclic Prefix
SVD	Singular Value Decomposition
ISI	Inter Symbol Interference
ICI	Inter carrier Interference
CA	Carrier Aggregation
LTE	Long Term Evolution
MSE	Mean Square Error
LMMSE	Least Minimum Mean Square Error
FFT	Fast Fourier Transform
IFFT	Inverse Fast Fourier Transform
CS	Compressive Sensing

VI. ACKNOWLEDGMENT

First and foremost, I thank GOD for his abundance grace and countless blessings in making this work a great success. I present my sincere thanks to my project supervisor, **Dr. D.SRIDHARAN, Professor**, Department of Electronics & Communication Engineering for his whole hearted support, patience, valuable guidance, technical expertise and encouragement in my project. Last but not the least, I would not have made this project without the support from my beloved **parents**. They encouraged me morally and took pride in what I achieved. They deserve my sincerest gratitude.

REFERENCES

[1]. "Spectrum policy task force, spectrum policy task force report," Federal Communications Commission ET, 2002. S. Haykin, "Cognitive radio: brain-empowered wireless communications," IEEE J. Sel. Areas Commun., vol. 23, no. 2, pp. 201–220, Feb. 2005.

[2]. R. Qiu, Z. Hu, H. Li, and M. Wicks, Cognitive Radio Communication and Networking: Principles and Practice. Wiley, 2012.

[3]. C. Yi and J. Cai, "Two-stage spectrum sharing with combinatorial auction and stackelberg game in recall-based cognitive radio networks," IEEE Trans. Commun., vol. 62, no. 11, pp. 3740–3752, Nov. 2014.

[4]. C. Yi and J. Cai, "Multi-item spectrum auction for recall-based cognitive radio networks with multiple heterogeneous secondary users," IEEE Trans. Veh. Technol., vol. 64, no. 2, pp. 781–792, Feb. 2015.

[5]. B. Van Veen and K. Buckley, "Beamforming: a versatile approach to spatial filtering," IEEE ASSP Mag., vol. 5, no. 2, pp. 4–24, Apr. 1988.

[6]. S. Yiu, M. Vu, and V. Tarokh, "Interference reduction by beamforming in cognitive networks," in Proc. IEEE Globecom, Nov. 2008, pp. 1–6.

[7]. R. Xie, F. Yu, and H. Ji, "Joint power allocation and beamforming with users selection for cognitive radio networks via discrete stochastic optimization," in Proc. IEEE Globecom, Dec. 2011, pp. 1–5.

[8]. B. Zayen, A. Hayar, and G. Oien, "Resource allocation for cognitive radio networks with a beamforming user selection strategy," in Signals, Syst. and Comput., Conf. Rec. of the Forty-Third Asilomar, Nov. 2009, pp. 544–549.

[9]. O. Abdulghfoor, M. Ismail, and R. Nordin, "Power allocation via interference compensation in underlay cognitive radio networks: A game theoretic perspective," in Int.l Symp. Telecommun. Tech. (ISTT), Nov 2012, pp. 296–301.

[10]. Zhongren Cao, U. Tureli, Yu-Dong Yao and P. Honan, "Frequency synchronization for generalized OFDMA uplink," IEEE Global Telecommunications Conference 2004, Nov. 2004.

[11]. Xiupei Zhang and Heung-Gyoon Ryu, "Joint Estimation and Suppression of Phase Noise and CFO in MIMO SC-FDMA with SCSFBC, been accepted for publishing in the IET Communications.

[12]. Xiupei Zhang and Heung-Gyoon Ryu, " Suppression of ICI and MAI in SC-FDMA Communication System with Carrier Frequency Offsets," IEEE Transaction on Consumer Electronics, vol.56, no.2, pp.359-365, May, 2010.

[13]. J.G. Andrews et al., "Femtocells: Past, present, and future," IEEE Journal on Selected Areas in Communications, vol. 30, no. 3, p. 497 508, Apr. 2012.

[14]. R.W. Heath et al., "A current perspective on distributed antenna systems for the downlink of cellular systems," IEEE Communications Magazine, vol. 51, no. 4, pp. 161 – 167, Apr. 2013.

[15]. G. Wunder et al., "5GNOW: non-orthogonal, asynchronous waveforms for future mobile applications," IEEE Communications Magazine, vol. 52, no. 2, pp. 97 – 105, Feb. 2014.

[16]. "System-Level Interfaces and Performance Evaluation Methodology for 5G Physical Layer Based on Non-orthogonal Waveforms," in Asilomar Conference on Signals, Systems and Computers, Nov. 2013, pp. 1659 – 1663.

[17]. Z. Pi and F. Khan, "An introduction to millimeter-wave mobile broadband systems," IEEE Communications Magazine, vol. 49, no. 6, pp. 101 – 107, Jun. 2011.

[18]. F. Rusek et al., "Scaling up MIMO: Opportunities and challenges with very large arrays," IEEE Signal Processing Magazine, vol. 30, no. 1, pp. 40 – 60, Jan.2013.

[19]. F. Boccardi et al., "Five Disruptive Technology Directions for 5G," IEEE Communications Magazine, vol. 52, no. 2, pp. 74 – 80, Feb. 2014.

[20]. G.P. Fettweis and S. Alamouti, "5G: Personal mobile internet beyond what cellular did to telephony," IEEE Communications Magazine, vol. 52, no. 2, pp. 140 – 145, Feb. 2014.

[21]. P. Rost et al., "Cloud technologies for flexible 5G radio access networks," IEEE Communications Magazine, vol. 52, no. 5, pp. 68–76, May 2014.

[22]. N. Ghazisaidi et al., "Fiber-wireless (FiWi) access networks: A survey," IEEE Communications Magazine, vol. 47, no. 2, pp. 160 – 167, Feb. 2009.